PHYSICAL REVIEW B VOLUME 4, NUMBER 4 15 AUGUST 1971

Computation of Raman-Scattering Cross Sections in Rare-Gas Crystals. II. Helium

N. R. Werthamer
Bell Telephone Laboratories, Murray Hill, New Jersey 07974

and

R. L. Gray
Bell Telephone Laboratories, Murray Hill, New Jersey 07974
and IBM Research Laboratories, San Jose, California 95114

and

T. R. Koehler
IBM Research Laboratories, San Jose, California 95114
(Received 13 April 1971)

One- and two-phonon Raman-scattering efficiencies are computed for the hcp phase of solid helium, following a theoretical model used previously for neon and argon. Attention is given to the dependence of the efficiencies on photon polarizations, photon energy loss, and crystal density. Two-phonon efficiencies are also computed for the bcc phase, and critical points are identified.

In a recent publication,[1] the first in this series, we presented computational results for two-phonon Raman scattering from solid fcc neon and argon, based[2] on a model of the solid as composed of neutral but dipole-polarizable point masses. As a continuation of this work, we present here Raman-scattering computations for helium in both the hcp and the bcc phase. In the hcp phase, where the structure has two atoms per unit cell, one-phonon scattering from the Raman-active transverse-optical branches is expected in addition to two-phonon scattering.

Just as in Ref. 1, we begin by adopting formula (31) of Ref. 2 for the two-phonon scattering efficiency at zero temperature. We also use formula (29) of Ref. 2 for the one-phonon efficiency. The phonon frequencies substituted into these formulas are those previously computed for the hcp phase by Gillis *et al.*,[3] and for the bcc phase by Koehler,[4] using the first-order self-consistent phonon scheme.

hcp LATTICE

If we write the two-phonon scattering efficiency as

$$S_2(\omega) \equiv \hat{\epsilon}_f \hat{\epsilon}_i : \underline{S}(\omega) : \hat{\epsilon}_f \hat{\epsilon}_i \,, \tag{1}$$

where $\hat{\epsilon}_{(f,i)}$ are the (final, incident) photon polarization unit vectors and ω is the loss of angular frequency to the crystal, then the fourth-rank tensor $\underline{S}(\omega)$ has the same symmetry properties as the elastic constant tensor. For the hcp lattice this implies that $\underline{S}(\omega)$ has no more than five independent elements, and we take these to be S_{11}, S_{13}, S_{33}, S_{44}, and S_{66} in the usual Voight notation. Then $S_2(\omega)$ can be written as

$$S_2(\omega) = S_{11}(\omega)(\vec{\epsilon}_{f\perp}\cdot\vec{\epsilon}_{i\perp})^2 + 2\,S_{13}(\omega)(\vec{\epsilon}_{f\perp}\cdot\vec{\epsilon}_{i\perp})(\vec{\epsilon}_{f\parallel}\cdot\vec{\epsilon}_{i\parallel}) + S_{33}(\omega)(\vec{\epsilon}_{f\parallel}\cdot\vec{\epsilon}_{i\parallel})^2 + S_{44}(\omega)\,|\vec{\epsilon}_{f\perp}\times\vec{\epsilon}_{i\perp}|^2 + S_{66}(\omega)\,|\vec{\epsilon}_{f\perp}\times\vec{\epsilon}_{i\parallel} - \vec{\epsilon}_{f\parallel}\times\vec{\epsilon}_{i\perp}|^2 \,, \tag{2}$$

where ($\perp$, $\parallel$) here denote (perpendicular, parallel) to the hexagonal c axis. However, as pointed out in Ref. 1, the assumption that electronic excitation is transferred between atoms only via dipole forces has the consequence that $\underline{S}(\omega)$ further obeys

$$\overleftrightarrow{1} : \underline{S}(\omega) = 0 \,. \tag{3}$$

Equation (3) leads in the case of the hcp lattice to the two further independent linear relations between the elements of $\underline{S}(\omega)$,

$$2S_{13}(\omega) + S_{33}(\omega) = 0 \tag{4a}$$

and

$$2S_{11}(\omega) + S_{13}(\omega) - 2S_{44}(\omega) = 0 \,. \tag{4b}$$

The number of independent elements is thus reduced to three, and we choose these to be S_{33}, S_{44}, and S_{66}. Then $S_2(\omega)$ can be further simplified to

$$S_2(\omega) = S_{33}(\omega)(\vec{\epsilon}_{f\parallel}\cdot\vec{\epsilon}_{i\parallel} - \tfrac{1}{2}\vec{\epsilon}_{f\perp}\cdot\vec{\epsilon}_{i\perp})^2 + S_{22}(\omega)\epsilon_{f\perp}{}^2\epsilon_{i\perp}{}^2 + S_{66}(\omega)\,|\vec{\epsilon}_{f\perp}\times\vec{\epsilon}_{i\parallel} - \vec{\epsilon}_{f\parallel}\times\vec{\epsilon}_{i\perp}|^2 \,. \tag{5}$$

Equation (5) appears to depend in a complicated way on the photon polarization vectors relative to the hexagonal axis, which might not seem easy to determine. However, the one-phonon scattering efficiency varies[2] with photon polarizations as

$$S_1(\omega) \propto \epsilon_{f\perp}^2 \epsilon_{i\perp}^2 . \tag{6}$$

This implies that a determination of the one-phonon scattering intensity as a function of polarization suffices to fix uniquely the c axis relative to the scattering axes, which in turn allows an unambiguous computation of the three scalar combinations appearing in Eq. (5) once $\hat{\epsilon}_f$ and $\hat{\epsilon}_i$ are given. Thus the one-phonon scattering is itself sufficient in determining the crystal orientation to obtain all tensor components of the two-phonon scattering.

The two-phonon efficiency in a polycrystalline sample is easily obtained by averaging Eq. (5) over all crystal orientations:

$$S_2(\omega)\big|_{\text{poly}} = \tfrac{3}{5}\left[\tfrac{1}{4} S_{33}(\omega) + \tfrac{2}{3} S_{44}(\omega) + \tfrac{2}{3} S_{66}(\omega)\right]\left[1 + \tfrac{1}{3}(\hat{\epsilon}_f \cdot \hat{\epsilon}_i)^2\right] . \tag{7}$$

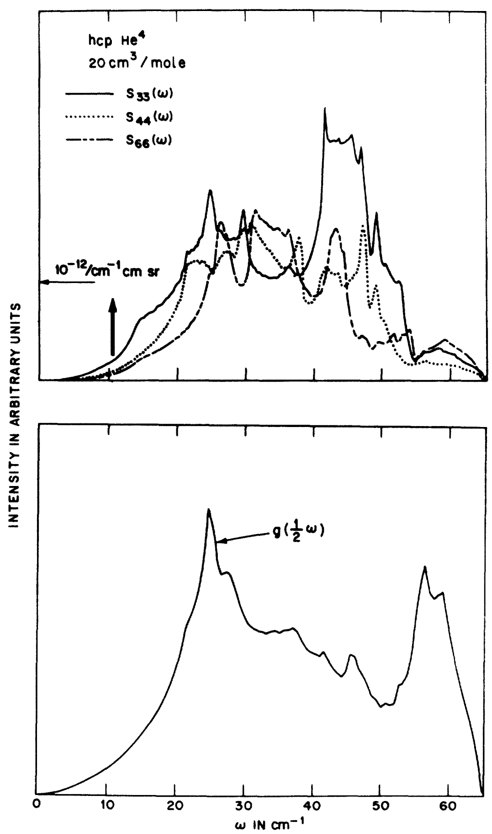

FIG. 1. Upper plot: Tensor components of two-phonon scattering efficiency, as a function of energy loss, for hcp He^4 at a molar volume of 20 cm^3. Horizontal arrow marks intensity level of 10^{-12}/cm^{-1} cm sr. Vertical arrow marks position of one-phonon scattering peak. Lower plot: One-phonon density of states, scaled by factor of 2 on the abscissa, to indicate identity of critical points in the two-phonon scattering.

Again, as in the cubic case,[1] the dependence on photon polarizations factors out from the lattice structure and dynamics. This property is actually a general one for any crystal structure, being a consequence merely of the dipole-transfer assumption [Eq. (3)].

Numerical techniques for computing the two-phonon efficiencies in hcp helium were similar to those previously employed[1] for fcc neon and argon. In the present case, 32 shells of nearest neighbors (radii up to four nearest-neighbor distances) were used in the direct lattice sums, while the reciprocal-lattice sums were performed over 17 921 inequivalent points in the irreducible $\frac{1}{24}$ of the first Brillouin zone. The one-phonon efficiencies were computed with 225 shells of nearest neighbors (radii up to eight nearest-neighbor distances), because of less rapid convergence of the matrix elements than in the two-phonon case. For assigning absolute physical units to the efficiencies, we use the values 0.2×10^{-24} cm^3 for the helium atomic polarizability, $\epsilon = 10.22$ K and $\sigma = 2.556\times10^{-8}$ cm for the Lennard-Jones 6-12 potential parameters, and $\Lambda = (0.1816,\ 0.2423)$ for the (He^4, He^3) de Boer parameter. We assume that the incident light beam is from the 4880-Å mode of the argon-ion laser.

The three efficiency components S_{33}, S_{44}, and S_{66} are plotted in Fig. 1 as a function of ω for the molar volume of 20 cm^3. In contrast to the situation for the fcc lattice, the three functions have a great deal of fine structure without much in the way of dominant characteristic features. For this reason we have not carried through an attempt to identify critical points in the two-phonon joint density of states. Furthermore, even just the one-phonon density of states in the hcp structure has a great sensitivity in its gross qualitative features to small changes in the effective force constants and the resulting dispersion curves. This can be seen in the remarkable differences of the one-phonon density of states, $g(\frac{1}{2}\omega)$ in Fig. 1, and sequence of the critical points between the analysis of neutron-scattering observations by Reese *et al.*[5] on hcp helium at 16 cm^3/mole, the calculations of Morley and Kliewer[6] at the same density, and our own computations (plotted in Fig. 1 for 20 cm^3/mole), even though the dispersion curves in all three instances differ by no more than 30% at worst. A similar disparity occurs in comparisons among three hcp metals analyzed by Raubenheimer and Gilat,[7] and between these metals and hcp helium. This great sensitivity of the hcp density of states contrasts with the situation in the fcc structure, where the argon and neon densities of states[1] differ only in minor ways from that of aluminum.[8] Thus we are not confident that our theoretical techniques for obtaining the phonon frequencies of hcp helium are sufficiently accurate as yet to give our results for S_2 as a function of ω quantitative reliability.

We do, however, have much more confidence in the total integrated intensities, defined as

$$\underline{S} \equiv \int_0^\infty d\omega\, \underline{S}(\omega) \; . \tag{8}$$

Values for S_{33}, S_{44}, and S_{66} are tabulated in Table I for He^4 at molar volumes of 16, 18, and 20 cm^3 and for He^3 at 18 cm^3. In addition, the integrated one-phonon intensity S_1 is also quoted. The magnitude of the efficiencies, while extremely small, does not rule out the possibility of detection by present-day experimental techniques. The requirement of averaging the matrix elements over the lattice zero-point motion reduces them by a factor of roughly 2 in helium, with a consequent reduction in the intensities by a factor of roughly 4. The two-phonon integrated efficiency is more than an order of magnitude larger than the one-phonon integrated efficiency (despite our earlier estimate[2] that the ratio would be an order of magnitude *smaller* due to an additional small factor of the dimensionless mean-square phonon amplitude for each phonon emitted) because the matrix elements for two-phonon emission are an order of magnitude larger than for one-phonon emission, which in turn arises from the much larger number of allowed intermediate states.

The density dependence of the efficiencies is of some interest, since it contrasts with previous estimates[1] for neon and argon. In the present case the two-phonon efficiencies follow the dependence $S_2 \propto a^{-7}$. These can be understood[2] on the basis of optical and zone-boundary phonon frequencies varying as a^{-4}, which is roughly the result of our computations,[3] at least in the molar volume range above 18 cm^3. These dependencies differ substantially from the case of neon and argon,[1] primarily because there the relevant phonon frequencies vary as a^{-7}. Our interpretation is that in neon and argon, where a cutoff on the short-range repulsive part of the potential is not needed, the short-wavelength phonons are determined primarily by the r^{-12} repulsive part of the Lennard-Jones potential; whereas in helium, with much larger amplitude of atomic vibrations, the phonon frequencies must be calculated including a Jastrow short-range cutoff function, which softens the repulsion sufficiently so that the phonons are determined much more by the r^{-6} attractive part of the potential. The difference may also be due in part to the much larger zero-point motion in helium than in neon or argon, which in turn expands the nearest-neighbor distance out well beyond the minimum point of the Lennard-Jones potential. Atomic motions centered about such an expanded spacing sample the attractive part of the potential in greater proportion to the repulsive part than do motions centered closer to the potential minimum. In any event, our analysis indicates that the density dependence of the scattering efficiencies is sensitive to the individual mode Grüneisen constants.

TABLE I. Integrated one-phonon efficiencies and two-phonon efficiency components, in units of $cm^{-1}\,sr^{-1}$, for He^4 and He^3 at various molar volumes.

	hcp He^4 16 cm^3	hcp He^4 18 cm^3	hcp He^4 20 cm^3	hcp He^3 18 cm^3
s_1	4.30×10^{-12}	3.29×10^{-12}	2.57×10^{-12}	3.77×10^{-12}
s_{33}	6.10×10^{-11}	4.99×10^{-11}	4.26×10^{-11}	5.82×10^{-11}
s_{44}	4.34×10^{-11}	3.53×10^{-11}	3.00×10^{-11}	4.15×10^{-11}
s_{66}	3.98×10^{-11}	3.27×10^{-11}	2.80×10^{-11}	3.79×10^{-11}

	bcc He^3 20 cm^3	bcc He^3 22 cm^3	bcc He^3 24 cm^3
s_{11}	1.280×10^{-11}	1.051×10^{-11}	0.878×10^{-11}
s_{44}	1.119×10^{-11}	0.918×10^{-11}	0.768×10^{-11}

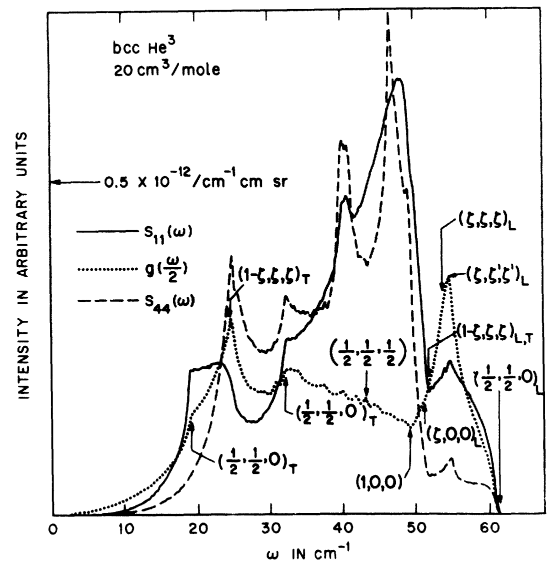

FIG. 2. Tensor components of two-phonon scattering efficiency, and one-phonon density of states suitably scaled, as a function of energy loss, for bcc He^3 at a molar volume of 18 cm^3. Horizontal arrow marks intensity level of $0.5\times10^{12}/cm^{-1}$ cm sr. Symmetry plane critical points in the one-phonon density of states are identified.

bcc LATTICE

Just as in the fcc lattice,[1] the tensor $\underline{S}(\omega)$ has only three independent elements by symmetry, and only two using the dipole-transfer assumption [Eq. (3)]. We take these to be $S_{11}(\omega)$ and $S_{44}(\omega)$, so that

$$S_2(\omega) = S_{11}(\omega)(\hat{\epsilon}_f \cdot \hat{\epsilon}_i)^2 + S_{44}(\omega)[1 - (\hat{\epsilon}_f \cdot \hat{\epsilon}_i)^2]$$
$$+ [4S_{44}(\omega) - 3S_{11}(\omega)][\epsilon_{fx}\epsilon_{fy}\epsilon_{ix}\epsilon_{iy} + \epsilon_{fy}\epsilon_{fz}\epsilon_{iy}\epsilon_{iz}$$

$$+\epsilon_{fz}\epsilon_{fx}\epsilon_{iz}\epsilon_{ix}] , \quad (9)$$

where x, y, z refer to components along cube axes. Numerical techniques for computing $S_{11}(\omega)$ and $S_{44}(\omega)$ were very similar to those described above for the hcp lattice.

Results for $S_{11}(\omega)$ and $S_{44}(\omega)$ as a function of ω, together with the one-phonon density of states $g(\frac{1}{2}\omega)$, are plotted in Fig. 2. The bcc lattice structure is simple enough that there are relatively few critical points, and these show up quite prominently in the two-phonon scattering. To identify the critical points, we have searched, via phonon-frequency isopleths, the three symmetry planes of the first Brillouin zone together with the zone face. All critical points found on these planes are labeled in Fig. 2, and it can be seen that these include most of the prominent ones. It also appears that there are additional critical points in the bcc spectrum which do not lie on any bounding plane of the irreducible $\frac{1}{48}$ of the Brillouin zone, and hence are not required by symmetry. We are not aware of any study specifying the minimum number, let alone their location, of critical points in the bcc structure.

[1]N. R. Werthamer, R. L. Gray, and T. R. Koehler, Phys. Rev. B 2, 4199 (1970).

[2]N. R. Werthamer, Phys. Rev. 185, 348 (1969).

[3]N. S. Gillis, T. R. Koehler, and N. R. Werthamer, Phys. Rev. 175, 1110 (1968).

[4]T. R. Koehler, Phys. Rev. Letters 18, 654 (1967).

[5]R. A. Reese, S. K. Sinha, T. O. Brun, and C. R. Tilford, Phys. Rev. A 3, 1688 (1971).

[6]G. L. Morley and K. L. Kliewer, Phys. Rev. 180, 245 (1969).

[7]L. J. Raubenheimer and G. Gilat, Phys. Rev. 157, 586 (1967).

[8]C. B. Walker, Phys. Rev. 103, 547 (1956).

PHYSICAL REVIEW B VOLUME 4, NUMBER 4 15 AUGUST 1971

Two-Electron F^- Centers in the Alkaline-Earth Fluorides

Herbert S. Bennett
National Bureau of Standards, Washington, D. C. 20234
(Received 9 April 1971)

The Hartree-Fock-Slater (HFS) equations for the two-electron orbitals localized about an anion vacancy in CaF_2, SrF_2, and BaF_2 have been solved numerically in the point-ion-lattice potential. It is found that the ground state $^1S(1s, 1s)$ contains bound electronic orbitals which are spatially compact. The existence of bound excited states for the F^- center in these crystals has been investigated. However, definitive statements on such excited states are not available at present.

I. INTRODUCTION

The F^- center in the alkaline-earth fluorides consists of two electrons, the defect electrons, localized about a vacant anion site.[1] Conclusive experimental evidence for the existence of the F^- center in CaF_2, SrF_2, and BaF_2 has not been reported in the literature.[2,3] This center has been proposed as one of several tentative models which might explain some of the many bands on the long-wavelength side of the M band in additively colored alkaline-earth fluorides. The M center consists of two F centers bound together at nearest-neighbor anion sites, and the F center consists of one electron localized about a vacant anion site. These give rise to the absorption bands which are formed during bleaching with F-band light. There are four bands situated in region from 600 nm (0.0760 a.u.) to 725 nm (0.0629 a.u.) for calcium fluoride and from 683 nm (0.0668 a.u.) to 805 nm (0.0566 a.u.) for strontium fluoride.[2,4] Only two bands have been observed on the long-wavelength side of the M band in barium fluoride. The bands which would correspond to the 805 and 775 nm bands in strontium fluoride have not been observed in barium fluoride because their intensities are too small.

F-band bleaching excites optically the F center, the M center, and other aggregate centers. Impurity centers such as rare earths are not considered in this paper. In the case of the alkali halide crystals, an excited defect electron of a color center may be assisted by thermal phonons into the conduction band. Once in the conduction band, it moves through the crystal until it is trapped again. The electron traps include ionized F^+ and M^+ centers and other ionized aggregate centers, and also the neutral F and M centers and other neutral aggregate centers. When an extra electron is trapped at a neutral center, a new center is formed. These centers are denoted, for example, by F^- and M^-,